Description of the low-lying collective states of ^{96}Zr based on the collective Bohr Hamiltonian including the triaxiality degree of freedom

E. V. Mardyban,[1,2] E. A. Kolganova,[1,2] T. M. Shneidman,[1,3] R. V. Jolos,[1,2] and N. Pietralla[4]

[1]*Joint Institute for Nuclear Research, 141980 Dubna, Moscow Region, Russia*

[2]*Dubna State University, 141982 Dubna, Moscow Region, Russia*

[3]*Kazan Federal University, Kazan 420008, Russia*

[4]*Institut für Kernphysik, TU Darmstadt, Schlossgartenstraße 9, D-64289, Darmstadt, Germany*

(Received 28 April 2020; accepted 18 August 2020; published 8 September 2020)

Background: Several collective low-lying states are observed in ^{96}Zr whose properties, which include excitation energies and $E2$, $E0$, and $M1$ transition probabilities, indicate that some of them belong to the spherical state and the other to deformed states. A consideration of these data in the full framework of the geometrical collective Model with both intrinsic shape variables, β and γ, and rotational degrees of freedom is necessary for ^{96}Zr.

Purpose: We investigate the properties of the low-lying collective states of ^{96}Zr based on the five-dimensional geometrical collective model including triaxiality as an active degree of freedom.

Method: The quadrupole-collective Bohr Hamiltonian, depending on both β and γ shape variables with a potential having spherical and deformed minima, is applied. The relative depth of two minima, height and width of the barrier, and rigidity of the potential near both minima are determined so as to achieve a satisfactory description of the observed properties of the low-lying collective quadrupole states of ^{96}Zr.

Results: It is shown that the low-energy structure of ^{96}Zr can be described in a satisfactory way within the geometrical collective model with a potential function supporting shape coexistence without other restrictions on its shape. It is shown that a correct determination of the β dependence of the collective potential from the experimental data requires a consideration in the framework of the full Bohr collective Hamiltonian. It is shown also that the excitation energy of the 2_2^+ state can be reproduced only if the rotation inertia coefficient is taken to be four times smaller than the vibrational one in the region of the deformed well. It is shown also that shell effects are important for the description of the $B(M1; 2_2^+ \to 2_1^+)$ and $B(M1; 3_1^+ \to 2_1^+)$ transition probabilities. An indication of the influence of the pairing vibrational mode on the $0_2^+ \to 0_1^+$ transition is confirmed, in agreement with the previous result.

Conclusion: Qualitative agreement with the experimental data on the excitation energies and $B(E2)$ and $B(M1; 2_2^+ \to 2_1^+)$ reduced transition probabilities is obtained.

DOI: 10.1103/PhysRevC.102.034308

I. INTRODUCTION

It has been well known for a long time that nuclei can exhibit both spherical and deformed shapes, including the intermediate region of nuclei transitional from spherical to deformed. What is more interesting is the phenomenon that a given nucleus can exhibit different shapes depending on the excitation energy. This phenomenon of shape coexistence has in recent years become the subject of many investigations in nuclear physics. Even more, shape coexistence is coming to be considered a near-universal property of nuclei [1]. A large number of papers, including reviews [1–4], are devoted to investigation of shape coexistence [5–20]. Various approaches have been employed to study this phenomenon [21–27].

Among different examples of shape coexistence, evidence of Zr isotopes' change of shape with excitation energy is especially interesting. Shape evolution can be characterized by a smooth or abrupt transition from spherical to deformed shape, and a significant or suppressed mixing of configurations with different shapes can take place. Such information is contained in electromagnetic transition probabilities, and a high purity of coexisting shapes has been established in ^{96}Zr [28].

In this paper we apply the geometrical collective-quadrupole model to a description of the properties of the low-lying states of ^{96}Zr including the shape coexistence phenomenon. Although an explanation of shape coexistence is a subject of microscopic nuclear modeling, the geometrical collective model deals directly with shape dynamical variables and, thus, may be capable of describing the dynamical consequences of shape coexistence and the properties of the collective low-lying states in general.

It is an open question whether a potential function in terms of shape variables can exist which allows for a reproduction of the data on the coexisting quadrupole collective structures of ^{96}Zr. The aim of the present paper is to investigate a possibility to describe, in principle, the properties of the low-lying collective states of ^{96}Zr and the amount of mixing of the configurations characterized by spherical and deformed

shapes based on the quadrupole collective Bohr Hamiltonian. It is also interesting in terms of what characteristics of the collective states shell effects are most pronounced.

II. HAMILTONIAN

The quadrupole-collective Bohr Hamiltonian can be written as [29]

$$H = -\frac{\hbar^2}{2\sqrt{\omega r}}\left(\frac{1}{\beta^4}\left[\frac{\partial}{\partial\beta}\sqrt{\frac{r}{\omega}}\beta^4 B_{\gamma\gamma}\frac{\partial}{\partial\beta} - \frac{\partial}{\partial\beta}\sqrt{\frac{r}{\omega}}\beta^3 B_{\beta\gamma}\frac{\partial}{\partial\gamma}\right]\right.$$
$$\left. + \frac{1}{\beta\sin 3\gamma}\left[-\frac{\partial}{\partial\gamma}\sqrt{\frac{r}{\omega}}\sin 3\gamma B_{\beta\gamma}\frac{\partial}{\partial\beta} + \frac{1}{\beta}\frac{\partial}{\partial\gamma}\sqrt{\frac{r}{\omega}}\sin 3\gamma B_{\beta\beta}\frac{\partial}{\partial\gamma}\right]\right) + \frac{1}{2}\sum_{k=1}^{3}\frac{\hat{J}_k^2}{\Im_k(\beta)} + V(\beta,\gamma), \quad (1)$$

where $\omega = B_{\beta\beta}B_{\gamma\gamma} - B_{\beta\gamma}^2$ is the determinant of the vibrational inertia tensor

$$B_{\text{vib}} = \begin{pmatrix} B_{\beta\beta} & \beta B_{\beta\gamma} \\ \beta B_{\beta\gamma} & \beta^2 B_{\gamma\gamma} \end{pmatrix}. \quad (2)$$

The moments of inertia $\Im_k$ with respect to the body-fixed axes are expressed as

$$\Im_k = 4B_k(\beta)\beta^2\sin^2\left(\gamma - \frac{2\pi k}{3}\right) \quad (3)$$

and $r = B_1B_2B_3$. The components of the angular momentum in the body-fixed frame are denoted as $\hat{J}_k$ and can be expressed in terms of the Euler angles. The potential energy is denoted as $V(\beta,\gamma)$. The Hamiltonian of Eq. (1) is a general case of the conventional Bohr Hamiltonian [30] allowing for nonzero value of $B_{\beta\gamma}$.

In the present work we aim to investigate whether it is possible to construct a potential energy in such a way that all existing data on the energies of the lowest angular momentum excited states and the transitions between these states will be described. Thus, it is not our task to minimize the number of parameters used to describe a potential function. Rather we want to find out how good, in principle, a description can be within the framework of the geometrical collective model of the nucleus with such an interesting structure as ^{96}Zr, in which both collective and shell effects are manifested. If such a potential can be constructed, will it describe the shape coexistence by having two minima, spherical and deformed? Previously in Ref. [31], this problem was solved under the assumption that the γ degrees of freedom can be separated from β in the potential and the value of γ is stabilized around $\gamma = 0^\circ$. This is obviously a rather crude approximation at least in the region of small values of β. In the present paper we avoid this assumption.

To simplify consideration, we make the following assumptions for the inertia coefficients:

$$B_{\beta\beta} = B_{\gamma\gamma} = B_0, \quad B_{\beta\gamma} = 0,$$
$$B_1(\beta) = B_2(\beta) = B_3(\beta) = b_{\text{rot}}(\beta)B_0, \quad (4)$$

where B_0 is the parameter scaling vibrational and rotational masses. Thus, the B_0 coefficient plays the role of the inertia parameter for vibrational modes throughout the β variation region. We accept this assumption, since the available experimental data on ^{96}Zr are not enough to extract from them information on the dependence of B_0 on the variables of the nuclear shape. Note, however, that such work was done, for example, for nuclei of the beginning of the rare earth region: ^{150}Nd, ^{152}Sm, and ^{154}Gd [32], where there are enough experimental data.

With respect to the value of the coefficient of inertia for rotational motion, however, it is known [33,34] that in deformed nuclei the rotational mass coefficient is 4–10 times smaller than the vibrational mass coefficients. For our consideration this means that in the region of the deformation minimum b_{rot} is much less than 1. In a complete correspondence with this result, it is shown below that in order to explain the excitation energy of the 2_2^+ state it is necessary to take b_{rot} several times less than unity. The average value of β^2 is about 20 times larger in the deformed states than in the spherical states. However, the level spacing between the 2^+ and the 0^+ states is only a factor of about 3 smaller in the deformed structure than in the spherical structure. This is the reason why we have to consider the reduction of b_{rot} from unity at vanishing deformation to a value of about 0.25 in the deformed minimum of the potential. Note, however, that since there is no experimental information on vibrational states whose wave functions are localized in the deformed minimum, it cannot be ruled out that not only the rotational, but also the total mass coefficient depends on deformation. Such a case was considered in [35–37]. Moreover, a question of the value of b_{rot} in the region of the spherical minimum remains open. The answer is given by the following consideration.

The collective Hamiltonian given in (1) is written in the internal coordinates. We can rewrite this Hamiltonian in term of the laboratory variables

$$\alpha_{2\mu} = D^2_{\mu 0}(\vec{\theta})\beta\cos\gamma + \frac{1}{\sqrt{2}}\left(D^2_{\mu 2}(\vec{\theta}) + D^2_{\mu -2}(\vec{\theta})\right)\beta\sin\gamma, \quad (5)$$

where $D^2_{\mu k}(\vec{\theta})$ is a Wigner function and $\vec{\theta}$ are Euler angles that characterize orientation of the internal coordinate system relative to the laboratory system. In the general case, the inertia tensor written in term of $\alpha_{2\mu}$ contains not only monopole, but also quadrupole and hexadecapole components [32]. Due to the presence of the last two components in the inertia tensor a difference between vibration and rotation coefficients of inertia arises in the deformed region. However, in the region of the spherical minimum the quadrupole and hexadecapole components are small because they are proportional to $\alpha_{2\mu}$, $(\alpha\alpha)_{2\mu}$, and $(\alpha\alpha)_{4\mu}$ and can be neglected, while the monopole

component contains a deformation-independent term. If only the monopole component of the inertia tensor is retained, the difference between vibrational and rotational inertia coefficients disappears. Therefore, we accept that in the region of the spherical minimum, where only vibrations with respect to the spherical shape are realized, $b_{\rm rot} = 1$. Note that the rotational moment of inertia $\Im_{\rm rot}$ is equal to $3b_{\rm rot}B_0\beta^2$, i.e., it is an increasing function of β.

Under the assumptions of Eq. (4), the Hamiltonian (1) takes the form

$$\hat{H} = -\frac{\hbar^2}{2B_0}\left(\frac{1}{b_{\rm rot}^{3/2}}\frac{1}{\beta^4}\frac{\partial}{\partial\beta}\beta^4 b_{\rm rot}^{3/2}\frac{\partial}{\partial\beta} + \frac{1}{\beta^2\sin 3\gamma}\frac{\partial}{\partial\gamma}\sin 3\gamma\right) + \frac{1}{2}\sum_{k=1}^{3}\frac{\hat{J}_k^2}{\Im_k(\beta)} + V(\beta,\gamma). \tag{6}$$

The potential energy $V(\beta,\gamma)$ is assumed to have two minima, spherical and deformed, separated by a barrier. This is in correspondence with the considerations [5,20] in the interacting boson model with configuration mixing (IBM-CM) where two configurations with different total number of bosons have been taken into account in order to include the effect of shape coexistence. We expect that the wave functions of the lowest excited states are localized in these minima while the weight of the function inside the barrier region is strongly suppressed. Therefore, it is reasonable to assume that the quantity $b_{\rm rot}$ has constant (but different) values in the regions of the spherical and deformed minima and the change from one value to another takes place in the region of the barrier. In this case, we can neglect a derivative of $b_{\rm rot}$ over β which is presented, in principle, in the kinetic part of the Hamiltonian (6), as it gives a nonzero contribution to the matrix elements of the Hamiltonian only in the barrier region where the wave functions are close to zero. Thus, we obtain finally the following model Hamiltonian:

$$H = -\frac{\hbar^2}{2B_0}\left(\frac{1}{\beta^4}\frac{\partial}{\partial\beta}\beta^4\frac{\partial}{\partial\beta} + \frac{1}{\beta^2\sin 3\gamma}\frac{\partial}{\partial\gamma}\sin 3\gamma\frac{\partial}{\partial\gamma} + \sum_{k=1}^{3}\frac{\hat{J}_k^2}{4b_{\rm rot}\beta^2\sin^2\left(\gamma-\frac{2\pi k}{3}\right)}\right) + V(\beta,\gamma), \tag{7}$$

where

$$b_{\rm rot} = \begin{cases} 1 & \text{if } \beta \leqslant \beta_m, \\ b_{\rm def} < 1 & \text{if } \beta > \beta_m. \end{cases} \tag{8}$$

The magnitude of the $b_{\rm rot}$ inside the deformed minimum is obtained by fitting the excitation energy of the 2_2^+ state. The change from the spherical to deformed value of $b_{\rm rot}$ occurs at $\beta = \beta_m$ which is taken around the maximum of the barrier separating spherical and deformed potential wells. Our calculations show that the precise value of β_m does not affect the qualitative results of the calculations.

To solve the eigenvalue problem with the Hamiltonian (7) we expand the eigenfunctions in terms of a complete set of basis functions that depend on the deformation variables β and γ and the Euler angles. These functions are well known and their construction is described in the literature. See, for instance, [38,39] and references below. For completeness of presentation we give some details here.

For each value of angular momentum I, the basis functions are written as

$$\Psi_{IM}^{n_\beta v\alpha} = R^{(n_\beta,v)}(\beta)\Upsilon_{v\alpha IM}(\gamma,\Omega), \tag{9}$$

where $\Upsilon_{v\alpha IM}$ is the SO(5) $\supset$ SO(3) spherical harmonics, which are the eigenfunctions of the operator $\hat{\Lambda}^2$:

$$\hat{\Lambda}^2\Upsilon_{v\alpha IM} = \left[-\frac{1}{\sin 3\gamma}\frac{\partial}{\partial\gamma}\sin 3\gamma\frac{\partial}{\partial\gamma} + \frac{1}{4}\sum_k\frac{\hat{J}_k^2}{\sin^2\left(\gamma-\frac{2\pi k}{3}\right)}\right]\Upsilon_{v\alpha IM} = v(v+3)\Upsilon_{v\alpha IM}. \tag{10}$$

In addition to the angular momentum I and its projection M, each function $\Upsilon_{v\alpha IM}$ is labeled by the SO(5) seniority quantum number v and a multiplicity index α, which is required for $v \geqslant 6$.

The $\Upsilon_{v\alpha IM}$ can be explicitly constructed as a sum over the states with explicit value of the projection K of the angular momentum on the intrinsic axis [40,41]:

$$\Upsilon_{v\alpha IM}(\gamma,\Omega) = \sum_{K=0,even}^{I} F_{v\alpha I,K}(\gamma)\xi_{KM}^I(\Omega), \tag{11}$$

where

$$\xi_{KM}^I(\Omega) = \frac{1}{\sqrt{2(1+\delta_{K0})}}\left[D_{MK}^I(\Omega)\right. \tag{12}$$

$$\left. + (-1)^I D_{M-K}^I(\Omega)\right] \tag{13}$$

and the $F_{v\alpha I,K}(\gamma)$ are polynomials constructed from the trigonometrical functions of γ [42].

The basis wave functions $R^{(n_\beta,v)}$ are chosen as the eigenfunctions of the harmonic oscillator Hamiltonian in β:

$$h_{h.o.} = \frac{1}{2}\left(-\frac{1}{\beta^4}\frac{\partial}{\partial\beta}\beta^4\frac{\partial}{\partial\beta} + \frac{v(v+3)}{\beta^2} + \frac{\beta^2}{\beta_0^4}\right). \tag{14}$$

The eigenfunctions of $h_{h.o.}$ have the following analytical form:

$$R_{n_\beta,v}(\beta) = N_\beta\left(\frac{\beta}{\beta_0}\right)^v L_{n_\beta}^{v+3/2}\left(\frac{\beta^2}{\beta_0^2}\right)\exp\left(-\frac{\beta^2}{2\beta_0^2}\right), \tag{15}$$

where β_0 is an oscillator length and the normalization constant N_β is given as

$$N_\beta = \sqrt{\frac{2n_\beta!}{\Gamma(n_\beta+v+5/2)}}. \tag{16}$$

The basis functions $R_{n_\beta,v}$ are completely specified by the choice of the oscillator length β_0. Our calculations have shown that the fastest convergence of the results is obtained when

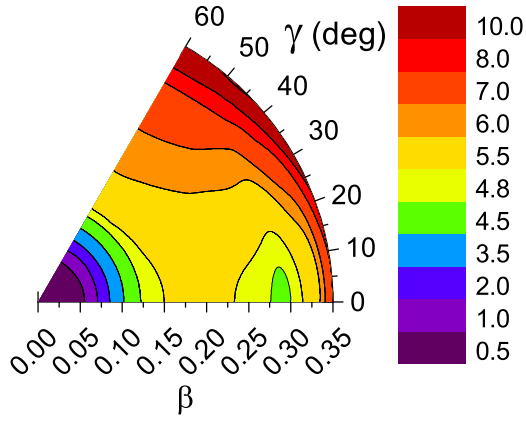

FIG. 1. Potential energy $V(\beta, \gamma)$ obtained in the calculations.

β_0 is chosen to be equal to the value at the region of the barrier separating spherical and deformed minima so that the oscillator potential coincides with the potential $V(\beta, \gamma = 0)$ at the top of the barrier. For such a choice of β_0, $(n_\beta)_{\max} = 30$ is enough to provide a convergence.

Diagonalization of the Hamiltonian (7) is realized in the basis of SO(5)-SO(3) spherical harmonics $\Upsilon_{v\alpha IM}(\gamma, \Omega)$ truncated to some maximum seniority $v_{\max}$. As shown in [43], taking $v_{\max} = 50$ is sufficient to provide a convergence of the calculation. A concrete realization of the construction of $\Upsilon_{v\alpha IM}(\gamma, \Omega)$ performed in [40,41] is used in the present work. These functions were first constructed in analytic form in [38] for $I \leqslant 6$.

The potential energy $V(\beta, \gamma)$ in (7) is chosen in the form

$$V(\beta, \gamma) = U(\beta) + C_\gamma \beta^3 (1 - \cos 3\gamma). \tag{17}$$

In (17), the deformed minimum of the potential energy is localized around $\gamma = 0$ for positive C_γ as assumed in our previous paper [31]. At the same time, this form of γ dependence of $V(\beta, \gamma)$ provides very weak γ dependence of $V(\beta, \gamma)$ at small β because of the factor β^3. The form of the potential energy at $\gamma = 0$ $[U(\beta)]$ and the parameter C_γ which determines the stiffness of the potential with respect to γ in the deformed minimum are fitted to reproduce the experimental data. As the first step, we have taken $U(\beta)$ as it was numerically determined in [31], $B_0 = 0.004$ MeV^{-1}, and $b_{\rm rot} = 0.2$ and performed calculations with different values of C_γ. We have found that $C_\gamma = 50$ MeV produces a reasonable value of the frequency of γ vibrations close to 1.5 MeV. No significant changes were found in the calculation results for the excitation energies and the $E2$ transition probabilities when C_γ was varied around 50 MeV.

As before in [31], to describe the shape of the axially symmetric part of the potential we defined several points fixing the positions of the spherical and deformed minima, the rigidity of the potential near its minima, and the height and width of the barrier separating two minima. The deformation at the second minimum has been taken to be $\beta = 0.24$ in agreement with the experimental value of $B(E2; 2_2^+ \to 0_2^+)$. The potential energy as a function of β is determined by using a spline interpolation between selected points. Then we solve numerically the Schrödinger equation with Hamiltonian (7), varying positions

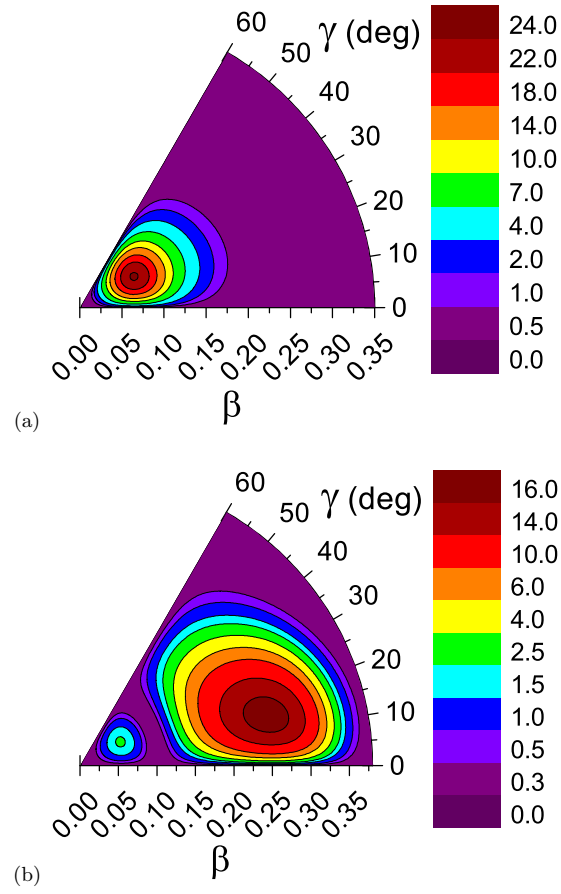

FIG. 2. The squares of the wave functions of the 0_1^+ (a) and 0_2^+ (b) states, multiplied by the volume element.

of the selected points in order to get a satisfactory description of the energies of the 2_1^+ and 2_2^+ states and the following transition probabilities: $B(E2; 2_2^+ \to 0_2^+)$, $B(E2; 2_1^+ \to 0_1^+)$, and $B(E2; 2_2^+ \to 0_1^+)$. The number of points is taken to be 16 to provide a smooth change of the potential. However, not all the points are of the same physical importance. In principle, the number of points can be minimized as, obviously, only the relative depths of the minima and the height and width of the barrier lead to physically meaningful changes. The mass parameter has been taken finally as $B_0 = 0.005$ MeV^{-1} to fix the energy of the 0_2^+ state.

The resulting potential $V(\beta, \gamma)$ is presented in Fig. 1. It is interesting that the inclusion of γ as a dynamical variable leads to a significant change of the shape of the potential in comparison to the case when γ was treated as a constant and not as a variable. The most important change occurs at the region of small β where the potential becomes shallower. In this region, the resulting potential is practically independent of γ and the wave function of the 0_1^+ state becomes independent of γ as well. This is not the case if γ is treated as a constant. This lack of the phase space results in the necessity to take a much deeper potential at small values of β to hold the wave function of 0_1^+ state inside the spherical minimum when γ is not considered dynamic.

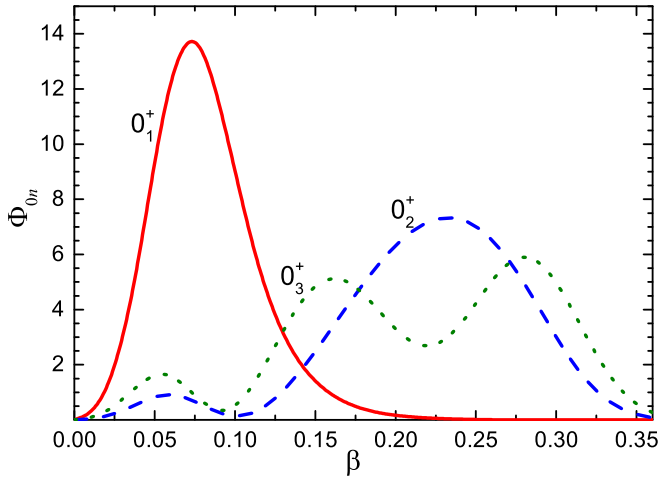

FIG. 3. Distribution over β of the squares of the wave functions of the 0_1^+ (solid line), 0_2^+ (dashed line), and 0_3^+ (dotted line) states calculated according (19).

III. RESULTS

The Hamiltonian eigenfunctions Ψ_{InM}, where I is the angular momentum, M is its projection and n is a multiplicity index, are obtained in calculations as a series expansions in the basic functions (9). However, for discussions below it is more convenient to present them in the basis of functions ξ^I_{KM} (12):

$$\Psi_{InM} = \sum_K \psi_{InK}(\beta,\gamma)\frac{1}{\sqrt{2(1+\delta_{K0})}}\big(D^I_{MK}(\Omega) + (-1)^I D^I_{M-K}(\Omega)\big). \quad (18)$$

We are using below the one-dimensional probability distributions over β which are obtained by integration of $|\Psi_{InM}|^2$ over γ and Euler angles,

$$\Phi_{In}(\beta) = \beta^4 \int_0^{\pi/3} \sin 3\gamma\, d\gamma \int d\Omega |\Psi_{InM}|^2, \quad (19)$$

and the weights of the wave functions in the spherical minimum W_{In} are determined as

$$W_{In} = \int_0^{\beta_m} d\beta\, \Phi_{In}(\beta), \quad (20)$$

where β_m is the position of the maximum of the barrier for $\gamma = 0$.

The calculated squares of the wave functions of the 0_1^+ and 0_2^+ states multiplied by the β- and γ-dependent volume element are presented in Fig. 2. One can see that the wave function of the 0_1^+ state is strongly localized in the spherical minimum. The wave function of the 0_2^+ state is mainly localized in the deformed minimum. Their spherical weights are $W_{0_1} = 0.985$ and $W_{0_2} = 0.136$ for 0_1^+ and 0_2^+ states, respectively. The fact that in Fig. 2 the squares of the wave functions are multiplied by the volume element that contains $\sin 3\gamma$ explains the shift of the maximum of the 0_2^+ wave function density to nonzero value of γ. The one-dimensional probability distribution over β which can be obtained by integrating $|\Psi^{n_\beta v\alpha}_{IM}|^2$ over γ and the Euler angles are presented in Fig. 3 for the 0_1^+ and 0_2^+ states.

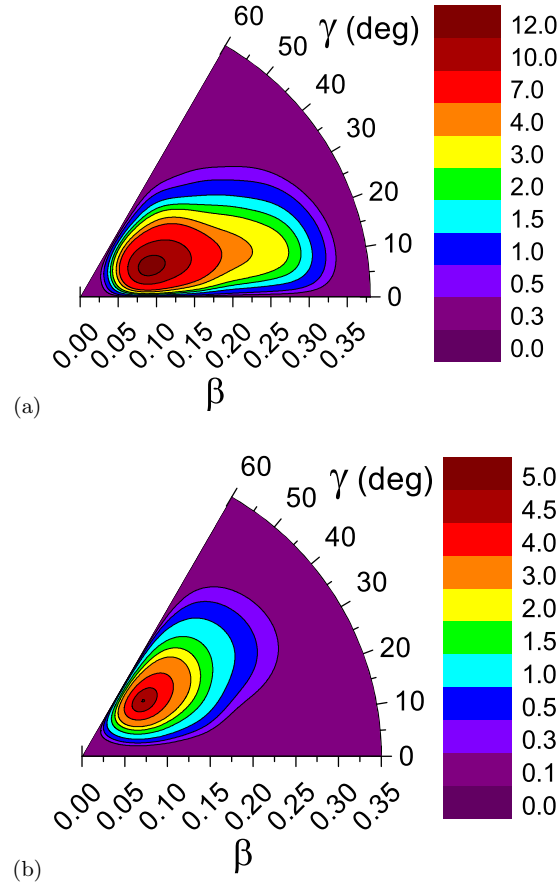

FIG. 4. The squares of the components of the wave function of the 2_1^+ state with $K = 0$ (a) and $K = 2$ (b) multiplied by the volume element.

For the lowest 2^+ states the situation is similar. The 2_1^+ state is localized in the spherical minimum with the weight $W(2_1^+) = 0.928$, while the second excited 2^+ state is only weakly presented there with $W(2_2^+) = 0.144$.

The wave functions of the 2^+ states have components with $K = 0$ and $K = 2$ determined by the expansion (18). The squares of the functions ψ_{2^+nK} for $K = 0$ and $K = 2$ multiplied by the volume element are presented in Fig. 4 for the 2_1^+ state and in Fig. 5 for the 2_2^+ state.

Using these wave functions the matrix elements of an arbitrary operator $\hat{F}$ can be calculated as

$$\langle f|\hat{F}|i\rangle = \int_0^\infty \beta^4 d\beta \int_0^{\pi/3} \sin 3\gamma\, d\gamma \int d\Omega\, \Psi_f^* \hat{F} \Psi_i. \quad (21)$$

We are particularly interested in calculations of the $E2$, $E0$, and $M1$ transition probabilities. The collective quadrupole operator responsible for $E2$ transitions is taken in the form

$$Q^{\rm coll}_{2\mu} = \frac{3Ze}{4\pi} R_0^2 \Big(\beta\cos\gamma D^2_{\mu 0}(\Omega) + \frac{1}{\sqrt{2}}\beta\sin\gamma\big[D^2_{\mu 2}(\Omega) + D^2_{\mu -2}(\Omega)\big]\Big), \quad (22)$$

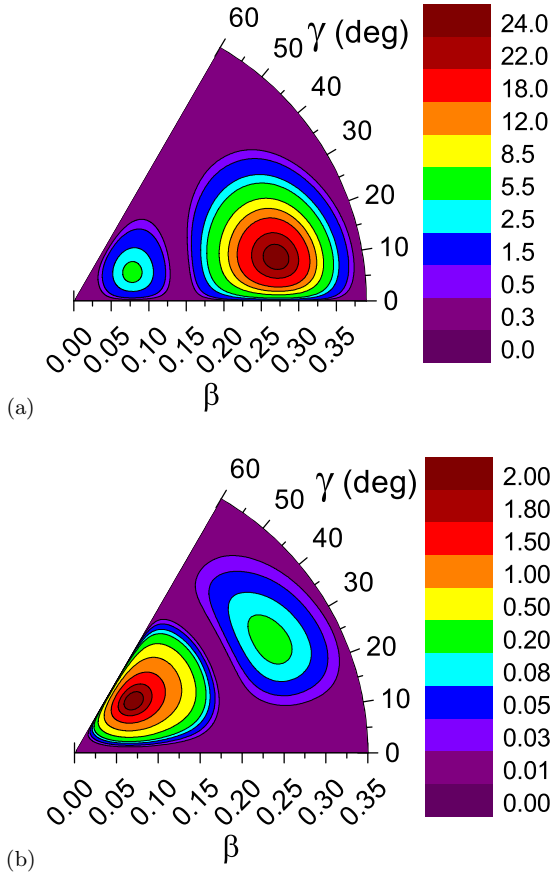

FIG. 5. The squares of the components of the wave function of the 2_2^+ state with $K = 0$ (a) and $K = 2$ (b) multiplied by the volume element.

where R_0 is the equivalent volume-conserving spherical radius of the nucleus and Z is the nuclear charge number. The $E0$ transition strength $\rho^2(0_2^+ \to 0_1^+)$ is calculated using the expression

$$\rho^2(0_2^+ \to 0_1^+) = \left(\frac{3Ze}{4\pi}\right)^2 |\langle 0_2^+|\beta^2|0_1^+\rangle|^2. \quad (23)$$

For the $M1$ transition operator we use the same expression as in [31]:

$$(M1)_\mu = \mu_N \sqrt{\frac{3}{4\pi}} g_R(\beta) I_\mu, \quad (24)$$

where μ_N is the nuclear magneton and $g_R(\beta)$ is the deformation-dependent collective g factor.

The results of calculations for the energies of the low-lying states and the electromagnetic transition probabilities are presented in Tables I and II together with the available experimental data. The root-mean-square deviation factor for the excitation energies (RMSD) is also presented in Table I.

Let us consider the results for the 0_3^+, 0_4^+, 2_3^+, and 4_1^+ excited states. The calculated energy of the 2_3^+ state exceeds the experimental value by 300 keV which is 10% of the total excitation energy of this state. The calculated value of $B(E2; 2_3^+ \to 2_1^+) = 10.6$ W.u. is quite collective, as is the experimental result. The experimental value [45] can vary between 0 and 120 W.u. depending on the quite uncertain lifetime of this level and on the unknown multipolarity of its decay transition to the 2_1^+ state. A distribution of the wave function of the 2_3^+ state over β, determined by (19), is presented in Fig. 6. It is seen that the component with $K = 0$

TABLE I. The calculated and the experimental energies of the low-lying 0^+, 2^+, 3^+, and 4^+ states. The experimental data are taken from [5,45].

State	$E_{\rm calc}$ (MeV)	$E_{\rm exp}$ (MeV)
$E(0_2^+)$	1.582	1.582
$E(0_3^+)$	2.443	2.695
$E(0_4^+)$	3.049	2.926
$E(2_1^+)$	1.724	1.750
$E(2_2^+)$	2.236	2.226
$E(2_3^+)$	2.974	2.669
$E(2_4^+)$	3.338	3.249
$E(3_1^+)$	2.653	2.439
$E(4_1^+)$	2.983	2.857
$E(4_2^+)$	3.447	3.082
RMSD (MeV)	0.194	

TABLE II. The calculated and the experimental values of the electromagnetic transition probabilities in ^{96}Zr. $B(E2)$ values are given in W.u., $B(M1)$ in nuclear magnetons. The value of $Q(2_2^+)$ is given in e b (electron barn). Experimental data are taken from [44,45].

Transition	Calc.	Expt.
$B(E2; 2_1^+ \to 0_1^+)$	5.23	2.3(3)
$B(E2; 2_2^+ \to 0_1^+)$	0.39	0.26(8)
$B(E2; 2_2^+ \to 0_2^+)$	26.0	36(11)
$B(E2; 2_2^+ \to 2_1^+)$	6.49	$2.8^{+1.5}_{-1.0}$
$B(E2; 3_1^+ \to 2_1^+)$	0.22	$0.1^{+0.3}_{-0.1}$
$B(E2; 3_1^+ \to 2_2^+)$	4.26	
$B(E2; 0_3^+ \to 2_1^+)$	1.14	
$B(E2; 0_3^+ \to 2_2^+)$	69.8	34(9)
$B(E2; 2_3^+ \to 2_1^+)$	10.6	50(70)
$B(E2; 2_3^+ \to 2_2^+)$	1.85	<400
$B(E2; 4_1^+ \to 2_1^+)$	16.7	16^{+5}_{-13}
$B(E2; 4_1^+ \to 2_2^+)$	43.0	56(44)
$B(E2; 4_1^+ \to 3_1^+)$	7.59	
$B(E2; 0_4^+ \to 2_1^+)$	0.36	0.3(3)
$B(E2; 0_4^+ \to 2_2^+)$	2.02	1.8(14)
$B(E2; 4_2^+ \to 2_1^+)$	4.82	
$B(E2; 4_2^+ \to 2_2^+)$	16.6	
$B(E2; 4_2^+ \to 3_1^+)$	0.07	
$B(E2; 2_4^+ \to 2_1^+)$	2.53	
$\rho^2(0_2^+ \to 0_1^+)$	0.0023	0.0075
$\rho^2(0_3^+ \to 0_1^+)$	0.001	0.004
$\rho^2(0_3^+ \to 0_2^+)$	0.038	0.0035
$B(M1; 2_2^+ \to 2_1^+)$	0.071	0.14(5)
$B(M1; 3_1^+ \to 2_1^+)$	0.0002	0.3(1)
$Q(2_2^+)$	−0.5	

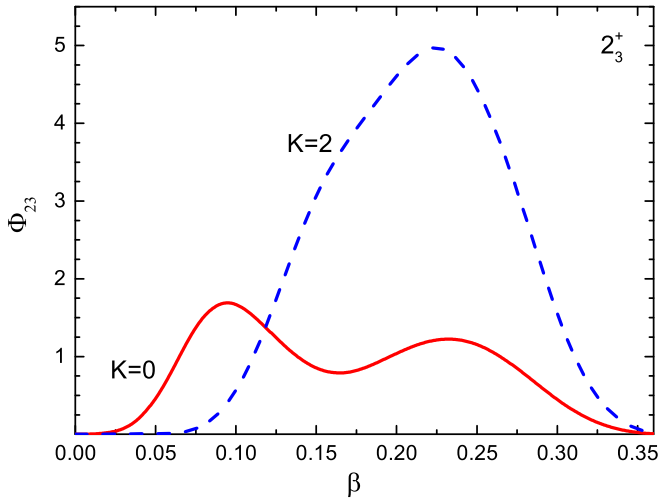

FIG. 6. Distribution over β of the squares of the components of the 2_3^+ state with $K = 0$ (solid line) and $K = 2$ (dashed line) calculated according to (19).

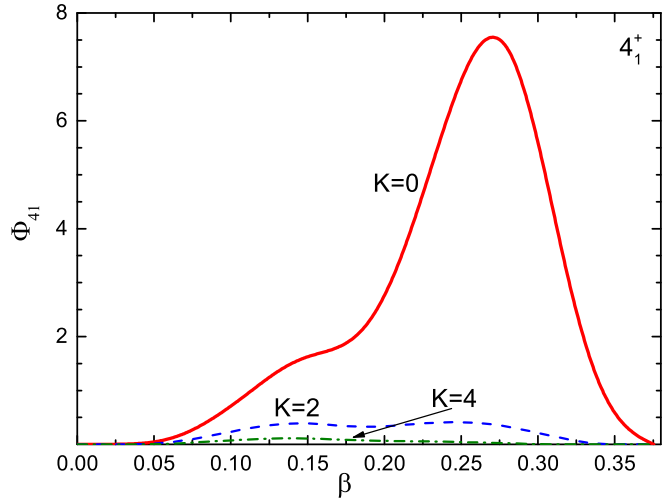

FIG. 7. Distribution over β of the squares of the components of the 4_1^+ state with $K = 0$ (solid), 2, and 4 (dot-dashed) calculated according to (19).

is almost equally distributed between the spherical and deformed minima. The component with $K = 2$ is predominantly located in the deformed minimum.

The experimental value of the excitation energy of the 3_1^+ state and the value of $B(E2; 3_1^+ \to 2_1^+)$ are reproduced by the calculations quite well. However, the experimental value of $B(M1; 3_1^+ \to 2_1^+) = 0.3\mu_N^2$ is too large to be reproduced in the framework of the collective model. For instance, the value of $B(M1; 3_\gamma^+ \to 2_\gamma^+)$ for transition between the states of the γ band in ^{168}Er is equal to $0.003\mu_N^2$ only, i.e., two orders of magnitude less than the value for ^{96}Zr. It could mean that the 3_1^+ state of ^{96}Zr has a large component of the shell model neutron configuration $(s_{1/2}^1 d_{5/2}^{-1})_3$ or even that its structure is almost exhausted by this configuration [44]. We mention, however, that the experimental value of $B(E2; 3_1^+ \to 2_1^+)$ can be reproduced only if both states have a collective admixture, since for the explanation of the experimental $B(E2; 3_1^+ \to 2_1^+)$ value the shell model neutron configurations $(s_{1/2}^1 d_{5/2}^{-1})_{2,3}$ requires a neutron $E2$ effective charge equal to 1. The calculated wave function of the 3_1^+ state is almost completely localized in the deformed minimum: $W_{3_1} = 0.96$.

The strong $E2$ transition between the 0_3^+ and the deformed 2_2^+ states is reproduced by our calculations because a significant part of the wave function of the 0_3^+ state is localized in the deformed minimum of the potential (see Fig. 3).

It is indicated in [44] that the 4^+ states at 2750 and 2781 keV presented in [45] have been observed in one experiment each only and were never confirmed. For this reason we disregard these states and compare the calculated characteristics of the 4_1^+ state with the experimental data for the 4^+ state observed at 2857 keV.

Our calculations reproduce the value of the very collective $E2$ transition $4_1^+ \to 2_2^+$, which shows that the significant part of the wave function of the 4_1^+ state is localized in the deformed minimum. This fact is confirmed by the distribution of the wave function of the 4_1^+ state shown in Fig. 7. It is seen also that the wave function of the 4_1^+ state is exhausted by the $K = 0$ component. The calculated ratio $B(E2; 4_1^+ \to 2_2^+)/B(E2; 2_2^+ \to 0_2^+) = 1.65$ is close to the Alaga value 1.43 for axially deformed nuclei. A distribution of the $K = 0$, 2, and 4 components of the wave function of the 4_1^+ state indicates that the large part of the total wave function is indeed located in the deformed minimum. At the same time the calculated $B(E2; 4_1^+ \to 2_1^+)$ value agrees within the limit of the experimental error with the observed value. The calculated ratio $[E(4_1^+) - E(0_2^+)]/[E(2_2^+) - E(0_2^+)]$ is equal to 2.14, which is close to the spherical limit. The experimental value of this ratio 1.98 practically coincides with the value for the spherical harmonic oscillator.

This astonishing apparent correspondence of the 4_1^+ state's properties to contradicting limits of the collective model can be understood from the following consideration. The dominant parts of the wave functions of the 2_2^+ and 4_1^+ states are located in the deformed minimum. However, smaller parts of the wave functions of these states are spread over the spherical minimum. This fact allows us to consider the 2_2^+ and 4_1^+ states as a mixture of the two dominant, lowest-lying spherical and deformed components, each. As a result of this mixing, the 4_1^+ state with dominantly deformed character is shifted down in energy because it is the lowest 4^+ state. At the same time, the predominantly deformed 2_2^+ state is shifted up in energy since it is the second excited 2^+ state. This lowering of the excitation energy of the 4^+ state and this increase of the 2^+ state's energy in the deformed well lead to the observed significant reduction of the $R_{4/2}$ ratio from the value of 10/3 expected for axially deformed nuclei towards a smaller value closer to 2.

Let us analyze the result obtained for $\rho^2(0_2^+ \to 0_1^+)$, which is by factor 3 smaller than the experimental value. The definition of the $\rho^2(0_2^+ \to 0_1^+)$ value is given in (23). In order to get an expression for $\langle 0_2^+|\beta^2|0_1\rangle$ in terms of the quantities whose values are known from other experiments, let us calculate the double commutator $[[H, \beta^2], \beta^2]$ using the Hamiltonian (6).

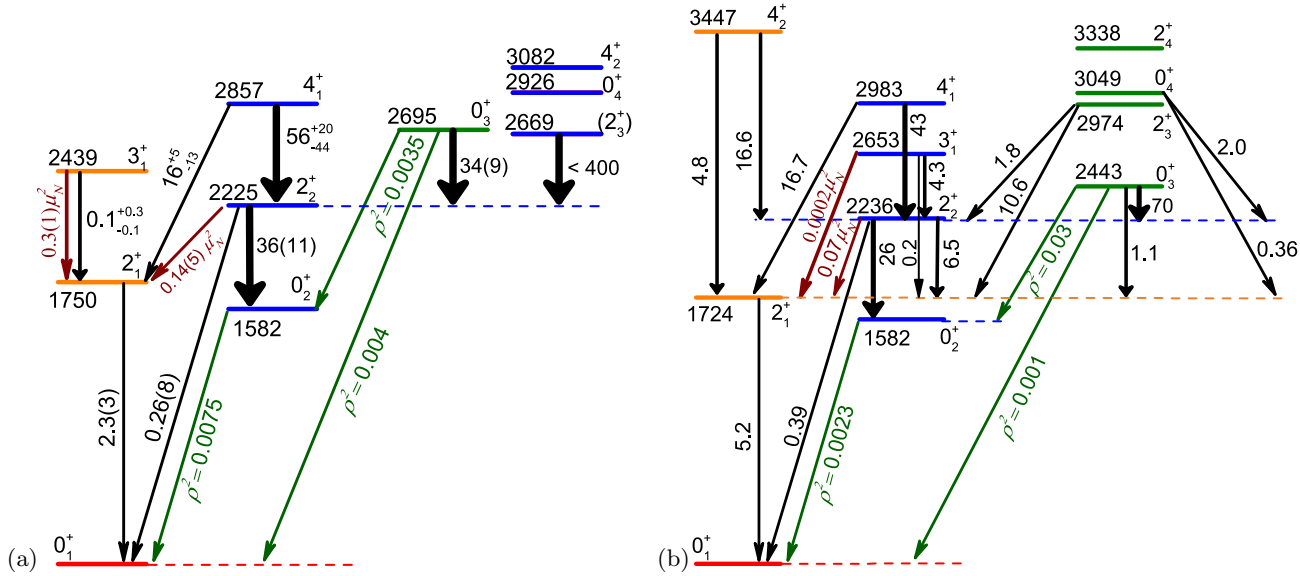

FIG. 8. Experimental (a) [44,45] and calculated (b) low-energy level schemes of positive-parity states of ^{96}Zr. Excitation energies are given in keV, $B(E2)$ transitions are given in W.u.

The result is

$$[[H,\beta^2],\beta^2] = \frac{4\hbar^2}{B_0}\beta^2. \tag{25}$$

Taking the average of (25) over the ground state 0_1^+ and assuming that the ground state is mainly related by $E0$ transition to the 0_2^+ state, we obtain

$$|\langle 0_2^+|\beta^2|0_1^+\rangle|^2 \leqslant \frac{2\hbar^2}{B_0}\langle 0_1^+|\beta^2|0_1^+\rangle\frac{1}{E(0_2^+)}, \tag{26}$$

where $E(0_2^+)$ is the excitation energy of the second 0^+ state. The sign of inequality in (26) appears because we neglect a contribution into the value of $\langle 0_1^+|\beta^2 H\beta^2|0_1^+\rangle$ of the other 0^+ states higher in energy than 0_2^+. The quantity $\langle 0_1^+|\beta^2|0_1^+\rangle$ can be expressed with good accuracy through the $B(E2;2_1^+\to 0_1^+)$ value using the collective model definition of the $E2$ transition operator:

$$\langle 0_1^+|\beta^2|0_1^+\rangle = \frac{5B(E2;2_1^+\to 0_1^+)}{\left(\frac{3}{4\pi}ZeR^2\right)^2}. \tag{27}$$

Substituting (26) and (27) into (23), we obtain

$$\rho^2(0_2^+\to 0_1^+) \leqslant \frac{\hbar^2}{B_0}\frac{1}{E(0_2^+)}\frac{10B(E2;2_1^+\to 0_1^+)}{e^2R^4}. \tag{28}$$

TABLE III. The calculated weights W_{In} in the spherical minimum of the considered states of ^{96}Zr.

State	W_{In}	State	W_{In}	State	W_{In}
0_1^+	0.985	0_2^+	0.136	0_3^+	0.292
2_1^+	0.772	2_2^+	0.182	2_3^+	0.289
4_2^+	0.636	4_1^+	0.139	0_4^+	0.202
		3_1^+	0.042	2_4^+	0.464

In our calculations the value of $\frac{\hbar^2}{B_0}$ was fixed as 5 keV in order to reproduce the experimental value of $E(0_2^+)$. Substituting this value and the calculated values of $E(0_2^+)$ and $B(E2;2_1^+\to 0_1^+)$ into (28), we obtain that

$$\rho^2(0_2^+\to 0_1^+) \leqslant 0.005, \tag{29}$$

in correspondence with the result given in Table I.

This result means that we cannot exclude that the pairing vibrational or some other modes play an important role in the description of the $E0$ transitions [46].

All experimental data on low-lying excited states of ^{96}Zr are presented in Fig. 8(a) and the corresponding calculation results are shown in Fig. 8(b). In both figures, states having very large spherical or deformed components are highlighted in two separate columns on the left. In Fig. 8(b) the division is based on the results of wave function weights W_{In} calculation which are shown in Table III. In contrast to the results [44] presented in Fig. 8(a) we placed the 4_2^+ state among the spherical and 3_1^+ state among the deformed ones based on the results shown in Table III.

IV. CONCLUSION

We have studied a possibility to describe the properties of the low-lying collective quadrupole states of ^{96}Zr basing on the Bohr collective Hamiltonian. Both β and γ shape collective variables are considered. The β dependence of the potential energy is fixed to describe the experimental data in the best possible way. However, the γ dependence of the potential is introduced in a simple way favoring axial symmetry at large β. The resulting potential has two minima, spherical and deformed, separated by a barrier.

Comparison of the β dependence of the potential defined in this paper with the potential defined in [31] shows how important it is to determine the potential from the analysis

of the experimental data based on the full Bohr collective Hamiltonian containing all five quadrupole dynamical variables. This consideration allows one also to obtain a more complete understanding of the wave functions of collective states, including the weights of the components with different K and their distribution in β-γ plane.

A degree of agreement of the results of calculations of excitation energies with experimental data is characterized by the root-mean-square deviation factor given in Table I. The results obtained for the reduced transition probabilities are mainly qualitatively consistent with the experimental data.

The 0_1^+, 2_1^+, and 4_2^+ states are calculated as rather pure vibrational states in a spherical or at most weakly deformed minimum, while the 0_2^+, 2_2^+, 3_1^+, and 4_1^+ states are dominated by prolate components with a little, although not vanishing, triaxiality. The experimental decay properties of the 3_1^+ state are, however, at variance with this solely geometrical interpretation. The calculations show that the wave function of the 3_1^+ state is located mainly in the deformed minimum. However, the experimental value of $B(M1; 3_1^+ \to 2_1^+)$ indicates the presence of the significant spherical component in the wave function of the 3_1^+ state. Thus, our calculations indicate a problem in description of the properties of the 3_1^+ state of ^{96}Zr in the framework of the geometrical collective model.

The calculated value of $\rho^2(0_2^+ \to 0_1^+)$ is around three times smaller than the measured value. This indicates an influence of the other degrees of freedom that is not included in the present consideration.

The rotational inertia coefficient is taken to be four times smaller than the vibrational one in order to reproduce the excitation energy of the 2_2^+ state. This is in accordance with the previously obtained indication that in deformed nuclei the vibrational and rotational inertia coefficients can differ bys several times.

ACKNOWLEDGMENTS

The authors express their gratitude to the RFBR (Grant No. 20–02-00176) and to the Heisenberg–Landau Program for support. One of the authors, T.M.S., acknowledges support from the Russian Government Subsidy Program of the Competitive Growth of Kazan Federal University. One of the authors, N.P., thanks A. Leviatan, T. Otsuka, V. Werner, and T. Beck for discussions and gratefully acknowledges support by the DFG under Grant No. SFB1245 and by the BMBF under Grants No. 05P19RDFN1 and No. 05P18RDEN9.

[1] K. Heyde and J. L. Wood, Rev. Mod. Phys. **83**, 1467 (2011).
[2] K. Heyde, P. Van Isacker, M. Waroquier, J. L. Wood, and R. A. Meyer, Phys. Rep. **102**, 291 (1983).
[3] J. L. Wood, K. Heyde, W. Nazarewich, M. Huyse, and P. V. Duppen, Phys. Rep. **215**, 101 (1992).
[4] A. Poves, J. Phys. G: Nucl. Part. Phys. **43**, 024010 (2016).
[5] J. E. García-Ramos and K. Heyde, Phys. Rev. C **100**, 044315 (2019).
[6] T. Togashi, Y. Tsunoda, T. Otsuka, and N. Shimizu, Phys. Rev. Lett. **117**, 172502 (2016).
[7] K. Sieja, F. Nowacki, K. Langanke, and G. Martínez-Pinedo, Phys. Rev. C **79**, 064310 (2009); **80**, 019905(E) (2009).
[8] J. E. García-Ramos, K. Heyde, R. Fossion, V. Hellemans, and S. De Baerdemacker, Eur. Phys. J. A **26**, 221 (2005).
[9] M. Böyükata, P. Van Isacker, and I. Uluer, J. Phys. G **37**, 105102 (2010).
[10] Y.-X. Liu, Y. Sun, X.-H. Zhou, Y.-H. Zhang, S.-Y. Yu, Y.-C. Yang, and H. Jin, Nucl. Phys. A **858**, 11 (2011).
[11] A. Petrovici, K. W. Schmid, and A. Faessler, J. Phys. Conf. Ser. **312**, 092051 (2011).
[12] R. Rodríguez-Guzmán, P. Sarriguren, L. M. Robledo, and S. Perez-Martin, Phys. Lett. B **691**, 202 (2010).
[13] J. Skalski, P.-H. Heenen, and P. Bonche, Nucl. Phys. A **559**, 221 (1993).
[14] J. Xiang, Z. P. Li, Z. X. Li, J. M. Yao, and J. Meng, Nucl. Phys. A **873**, 1 (2012).
[15] H. Mei, J. Xiang, J. M. Yao, Z. P. Li, and J. Meng, Phys. Rev. C **85**, 034321 (2012).
[16] J. Skalski, S. Mizutori, and W. Nazarewicz, Nucl. Phys. **617**, 282 (1997).
[17] C. Özen and D. J. Dean, Phys. Rev. C **73**, 014302 (2006).
[18] H. T. Fortune, Phys. Rev. C **95**, 054313 (2017).
[19] M. Büscher, R. F. Casten, R. L. Gill, R. Schuhmann, J. A. Winger, H. Mach, M. Moszyński, and K. Sistemich, Phys. Rev. C **41**, 1115 (1990).
[20] N. Gavrielov, A. Leviatan, and F. Iachello, Phys. Rev. C **99**, 064324 (2019).
[21] M. Bender, P.-H. Heenen, and P.-G. Reinhardt, Rev. Mod. Phys. **75**, 121 (2003).
[22] T. Niksic, D. Vretenar, and P. Ring, Prog. Part. Nucl. Phys. **66**, 519 (2011).
[23] P. Federman, S. Pittel, and R. Campos, Phys. Lett. B **82**, 9 (1979).
[24] K. Heyde, E. D. Kirchuk, and P. Federman, Phys. Rev. C **38**, 984 (1988).
[25] A. Etchegoyen, P. Federman, and E. G. Vergini, Phys. Rev. C **39**, 1130 (1989).
[26] A. Holt, T. Engeland, M. Hjorth-Jensen, and E. Osnes, Phys. Rev. C **61**, 064318 (2000).
[27] T. Niksic, D. Vretenar, G. A. Lalazissis, and P. Ring, Phys. Rev. Lett. **99**, 092502 (2007).
[28] C. Kremer, S. Aslanidou, S. Bassauer, M. Hilcker, A. Krugmann, P. von Neumann-Cosel, T. Otsuka, N. Pietralla, V. Yu. Ponomarev, N. Shimizu, M. Singer, G. Steinhilber, T. Togashi, Y. Tsunoda, V. Werner, and M. Zweidinger, Phys. Rev. Lett. **117**, 172503 (2016).
[29] T. Niksic, Z. P. Li, D. Vretenar, L. Prochniak, J. Meng, and P. Ring, Phys. Rev. C **79**, 034303 (2009).
[30] A. Bohr, Dan. Mat. Fys. Medd. Vid. Selsk. **26**(14), 1 (1952).
[31] D. A. Sazonov, E. A. Kolganova, T. M. Shneidman, R. V. Jolos, N. Pietralla, and W. Witt, Phys. Rev. C **99**, 031304(R) (2019).
[32] R. V. Jolos and P. von Brentano, Phys. Rev. C **79**, 044310 (2009).

[33] R. V. Jolos and P. von Brentano, Phys. Rev. C **76**, 024309 (2007).
[34] R. V. Jolos and P. von Brentano, Phys. Rev. C **77**, 064317 (2008).
[35] D. Bonatsos, P. Georgoudis, D. Lenis, N. Minkov, and C. Quesne, Phys. Lett. B **683**, 264 (2010).
[36] D. Bonatsos, P. E. Georgoudis, D. Lenis, N. Minkov, and C. Quesne, Phys. Rev. C **83**, 044321 (2011).
[37] D. Bonatsos, P. E. Georgoudis, N. Minkov, D. Petrellis, and C. Quesne, Phys. Rev. C **88**, 034316 (2013).
[38] D. R. Bes, Nucl. Phys. **10**, 373 (1959).
[39] G. G. Dussel and D. Bes, Nucl. Phys. A **143**, 623 (1970).
[40] D. J. Rowe, P. S. Turner, and J. Repka, J. Math. Phys. **45**, 2761 (2004).
[41] M. A. Caprio, D. J. Rowe, and T. A. Welsh, Comput. Phys. Commun. **180**, 1150 (2009).
[42] D. J. Rowe and J. L. Wood, *Fundamentals of Nuclear Models: Foundational Models* (World Scientific, Singapore, 2010).
[43] M. A. Caprio, Phys. Rev. C **83**, 064309 (2011).
[44] W. Witt, N. Pietralla, V. Werner, and T. Beck, Eur. Phys. J. A **55**, 79 (2019).
[45] https://www.nndc.bnl.gov/ensdf/
[46] S. Iwasaki, T. Marumori, F. Sakata, and K. Takada, Prog. Theor. Phys. **56**, 1140 (1976).